

# Ferromagnetism in a Realistic Two-Band Model: A Slave-Boson Study

Raymond Frésard<sup>§†</sup> and Mathieu Lamboley<sup>§‡</sup>

<sup>§</sup>*Institut de Physique, Université de Neuchâtel, A.-L. Breguet 1, 2000 Neuchâtel, Switzerland*

<sup>†</sup>*Laboratoire Crismat, UMR 6508 du Centre National de la Recherche Scientifique et de l'Institut des Sciences de la Matière et du Rayonnement, 6, Bld. du Maréchal Juin, 14050 Caen Cedex, France*

<sup>‡</sup>*Laboratoire de Génie Médical, EPFL, PSE A, 1015 Lausanne, Switzerland*

*Using a slave boson representation of multi-band Hubbard models, we investigate a two-band model relevant to layered perovskites in the vicinity of half-filling. Beside the strong influence of the Hund's rule coupling, we obtain that the phase diagram separates into two regions: a weak to moderate coupling region where the effective mass is weakly renormalized, and a strong coupling regime where it is strongly renormalized. The transition between these two regimes is very sharp. It takes place in a (vanishingly) small domain. A ferromagnetic instability is only found in the strongly correlated regime, and is triggered by the Hund's rule coupling. The results are compared to La-doped layered ruthenates.*

*PACS numbers: 71.10.Fd, 71.30.h, 74.70.Pq, 75.30.Kz.*

## 1. INTRODUCTION

The richness of the phase diagram of the Ruddlesden-Popper series of the ruthenates makes it a fascinating topic of current solid state physics. Indeed single-layered ruthenates can be a superconductor ( $\text{Sr}_2\text{RuO}_4$ ) as discovered by Maeno *et al.*<sup>1</sup> or an anti-ferromagnetic insulator ( $\text{Ca}_2\text{RuO}_4$ ), while multi-layered compounds may be ferromagnetic metals ( $\text{SrRuO}_3$  and possibly  $\text{Sr}_3\text{Ru}_2\text{O}_7$ ) or an anti-ferromagnetic metal ( $\text{CaRuO}_3$ ). This richness is particularly amazing when one observes that all these compounds are, from a theoretical point of view, remarkably similar. Indeed Ca and Sr

\*Dedicated to Peter Wölfe on the occasion of his 60th birthday.

are divalent cations, the electron-electron interaction is strongest on the Ru atoms, which are common to all compounds, and the lattice structure does not drastically change when scanning through this family. Nevertheless these small changes must be responsible for the variety of the ground states. This thus calls for an accurate description of the electronic band structure, for instance on the level of the tight binding approximation. Note that  $\text{Ca}_2\text{RuO}_4$  appears to be a Mott insulator below 300 K. Indeed, transport<sup>2</sup> and optical<sup>3</sup> measurements reveal a narrow gap of about 0.2 eV. It orders magnetically below  $T_N = 100$  K, and therefore the insulating state may not be attributed to the magnetic ordering.

Another striking feature is provided by La doping (or other trivalent cations) of both Sr- and Ca-based single layered compounds: in both cases a few percent doping turns these systems into ferromagnets<sup>4,5</sup>. For the Ca-based compound, the Curie temperature is about 100 K, while substitutions of Ca with other trivalent dopants, such as Y, Ce or Pr result in ferromagnetic states with Curie temperatures varying from 120 to 200 K<sup>4,6</sup>. For the Sr-based compound, La substitution results into a ferromagnetic state, with a Curie temperature of 40 K at a concentration of 4 percent of dopant<sup>5</sup>.

Instead of investigating the nature and the cause of the superconductivity in  $\text{Sr}_2\text{RuO}_4$ , which is still a controversial matter<sup>7,8,9,10,11</sup>, we rather concentrate on the Fermi liquid parameters and the magnetic structure of the entire series. The paper is organized as follows: we first introduce a model meant to capture the main feature of this series on a minimal model level. It includes the details of the band structure, inspired by a proposition from Noce and Cuoco<sup>12</sup> which is compatible with the experimentally determined Fermi surface<sup>13</sup> and spectroscopic data<sup>14</sup>. With minimal changes it can be applied to other perovskites such as vanadates and chromites. Secondly we explain how we are dealing with the strong Coulomb and Hund's rule couplings. Thirdly we present numerical results pointing towards a picture where both Ca-, and Sr-based ruthenates derive from a Mott insulator. The former system appears to be a Mott insulator at commensurate filling, while the second one should rather be seen as a self-doped Mott insulator. This is due to a partial filling of all sub-bands.

## 2. THE MODEL

### 2.1. Band Structure

The band structure of  $\text{Sr}_2\text{RuO}_4$  has been determined in the LDA by Oguchi<sup>15</sup> and Singh<sup>16</sup>. Later on it turned out that it can accurately be reproduced by a simple tight binding model by Noce and Cuoco<sup>12</sup>. The

### Ferromagnetism in a Realistic Two-Band Model.

bands which are crossing the Fermi energy are involving the three 4d  $t_{2g}$  orbitals of Ru, which are hybridizing with the 2p orbitals of O. They are filled with 16 electrons per  $\text{RuO}_2$  unit. Since the  $\text{RuO}_6$  octahedra are elongated along the z-direction, the  $d_{xy}$  orbital energy level is lying lower than the other two. From the LDA calculation, the corresponding band is nearly filled. In the following it will be neglected, except for possibly contributing to self-doping effects. The  $d_{x(y)z}$  orbitals hybridize only with the  $p_{x(y)}$  orbital of the neighboring O along the z-axis, and with the  $p_z$  orbital along the x (y)-axis. On top, the latter two orbitals weakly couple to one another as well. It numerically turns out that the dispersion in the z-direction is small, and will therefore be neglected. The resulting dispersions are given by the eigenvalues of:

$$H_z = \sum_{k,\sigma} \Psi_{k,\sigma}^\dagger \begin{pmatrix} \epsilon_d & 0 & -ie_k & 0 \\ 0 & \epsilon_d & 0 & -if_k \\ ie_k & 0 & \epsilon_p & a_k \\ 0 & if_k & a_k & \epsilon_p \end{pmatrix} \Psi_{k,\sigma}, \quad (1)$$

with  $\Psi_{k,\sigma}^\dagger = (d_{xz}^\dagger, d_{yz}^\dagger, p_{1z}^\dagger, p_{2z}^\dagger)_{k,\sigma}$ , and  $a_k = -4t_3 \cos\left(\frac{k_x a}{2}\right) \cos\left(\frac{k_y a}{2}\right)$ ,  $e_k = 2t_5 \sin\left(\frac{k_x a}{2}\right)$ , and  $f_k = 2t_5 \sin\left(\frac{k_y a}{2}\right)$ . Here  $-\frac{2\pi}{a} \leq k_x(k_y) \leq \frac{2\pi}{a}$  and  $a$  represents the lattice constant (the Ru-Ru distance). It is from now on set to unity. The LDA dispersions is best reproduced with the parameter set  $t_3 = 0.1 \text{ eV}$ ,  $t_5 = 0.85 \text{ eV}$ ,  $\epsilon_p = -2.4 \text{ eV}$  and  $\epsilon_d = -0.9 \text{ eV}$ . Integrating out the oxygen bands, and neglecting their frequency dependence, yields the effective model:

$$H_0 = \sum_{k,\sigma} (d_{xz,\sigma}^\dagger, d_{yz,\sigma}^\dagger) \begin{pmatrix} \tilde{e}_k & \tilde{a}_k \\ \tilde{a}_k & \tilde{f}_k \end{pmatrix} \begin{pmatrix} d_{xz,\sigma} \\ d_{yz,\sigma} \end{pmatrix}, \quad (2)$$

up to a constant energy shift. Here we introduced:  $\tilde{a}_k = -4t' \sin k_x \sin k_y$ ,  $\tilde{e}_k = t \cos k_x$ , and  $\tilde{f}_k = t \cos k_y$ . The effective hoppings  $t$  and  $t'$  are related to the original parameters by  $t = 2\frac{t_5^2}{\epsilon_p}$  and  $t' = t_3 \left(\frac{t_5}{\epsilon_p}\right)^2$ . Note that the two-dimensional character of the dispersions

$$E_{k,\nu,\sigma} = \frac{1}{2} (\tilde{e}_k + \tilde{f}_k) + \frac{1}{2} \nu \sqrt{(\tilde{e}_k - \tilde{f}_k)^2 + 4\tilde{a}_k^2}, \quad (3)$$

with  $\nu = \pm 1$ , purely follows from the off-diagonal terms. These two eigenvalues yield the dispersion one obtains in LDA calculation<sup>12</sup>. The resulting density of states is symmetrical with respect to half band filling, where it has a minimum. The band width  $W$  is 1.2 eV.

## 2.2. Interaction Terms

We have modeled the Coulomb interaction using a Hubbard  $U$ -term and Hund's rule coupling term  $J_H$ -terms, yielding the local Hamiltonian:

$$\begin{aligned}
 H_{int} = & U \sum_{i,\sigma,\rho'<\rho} n_{i,\rho,\sigma} n_{i,\rho',\sigma} \\
 & + U_1 \sum_{i,\rho' \neq \rho} n_{i,\rho,\uparrow} n_{i,\rho',\downarrow} + U_3 \sum_{i,\rho} n_{i,\rho,\uparrow} n_{i,\rho,\downarrow},
 \end{aligned} \tag{4}$$

where  $\sigma$  ( $\rho$ ) is a spin (band) index. The relation between the coefficients

$$U_n \equiv U + nJ_H \tag{5}$$

holds for perfect cubic symmetry<sup>17,18</sup>, otherwise one should work with the matrix elements  $F_0$ ,  $F_2$ , and  $F_4$ <sup>19</sup>. In the following we nevertheless stick to the minimal model using the relation Eq. (5). This amounts to deal with the parameters  $U$ ,  $J_H$ ,  $t$ , and  $t'$  (with  $t$  setting the energy scale). Since the ruthenates  $(\text{Sr}_{1-x}\text{Ca}_x)_2\text{RuO}_4$  may be Mott insulators (depending on the value of  $x$ ), perturbative calculations may be problematic. Here we resort to a slave boson approach<sup>20,19,21</sup>, which is the generalization of the Kotliar and Ruckenstein representation of the Hubbard model<sup>22</sup>, to the multi-band model. At this stage one may wish to introduce a rotation invariant formulation in the spirit of Li *et al.* or Frésard and Wölfle's representations<sup>23,24</sup>. In the one-band model, such a representation turned out to be necessary to obtain the correct contribution of the spin fluctuations to the specific heat on the one-loop level<sup>23</sup>. It also appeared very useful when investigate incommensurate states<sup>25,26,27</sup>. In the systems under consideration, perfect cubic symmetry is absent, and therefore rotational symmetry in spin space is not a requirement. Thus the local model Eq. (4) can be viewed as a model in its own right, despite of lacking rotational invariance. Note that the tightly related Gutzwiller Approximation has been suitably generalized to deal with rotationally symmetrical models<sup>18</sup>. Manifestly anti-ferromagnetic solutions are playing a role as well, as discussed by Hasegawa<sup>28</sup>. This is however a less puzzling issue than the occurrence of ferromagnetism, and is therefore not investigated here. Since there is no van Hove singularity at half-filling, we expect that an anti-ferromagnetic instability can only occur above a finite (and substantial)  $U$ , as it happens in the  $t - t' - U$  model<sup>29</sup> or in the one band model on the hexagonal lattice<sup>30</sup>. Recently Hasegawa<sup>31</sup> showed that orbitally ordered states in this model seem to rather appear for negative  $J_H$ .

In the slave boson approach to the multi-band model one introduces one slave boson field for each of the sixteen atomic configurations, and four

### Ferromagnetism in a Realistic Two-Band Model.

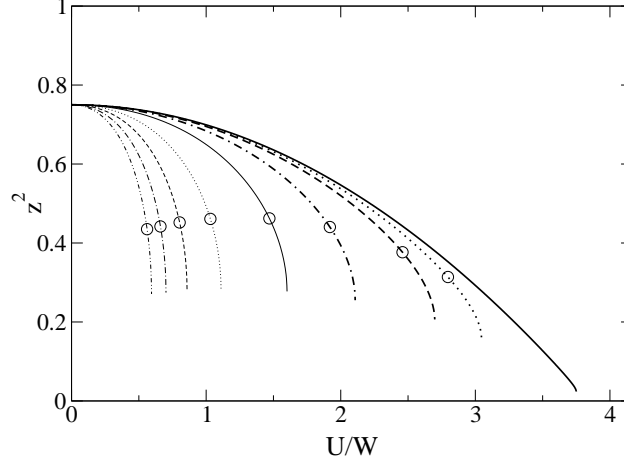


Fig. 1. Effective mass renormalization at  $\rho = 2$  for  $J_H/U = 0$  (thick full line), 0.01. (thick dotted line), 0.02 (thick dashed line), 0.05 (thick dashed-dotted line), 0.1 (thin full line), 0.2. (thin dotted line), 0.3 (thin dashed line), 0.4 (thin dashed-dotted line) and 0.5 (thin dashed-dotted-dotted line). The circles indicate the location of the first order transition.

auxiliary fermionic fields  $f_\alpha$  ( $\alpha$  being a composite spin and band index) as :

$$\begin{aligned}
 |\alpha\rangle &= p_\alpha^\dagger f_\alpha^\dagger |vac\rangle, \\
 |\alpha, \alpha'\rangle &= d_{\alpha\alpha'}^\dagger f_\alpha^\dagger f_{\alpha'}^\dagger |vac\rangle, \\
 |\alpha, \alpha', \alpha''\rangle &= t_{\alpha\alpha'\alpha''}^\dagger f_\alpha^\dagger f_{\alpha'}^\dagger f_{\alpha''}^\dagger |vac\rangle.
 \end{aligned} \tag{6}$$

On top of those, there is a boson  $e$  related to empty sites, and a boson  $q$  related to four-fold occupied sites. The original fermionic operators  $c_{i\alpha}^\dagger$  are expressed in terms of the auxiliary fields as  $c_{i\alpha}^\dagger = z_{i\alpha}^\dagger f_{i\alpha}^\dagger$  with  $z^\dagger$  given by Eq. (4-5) of Ref. 19, while the constraints linking the auxiliary fields are given by Eq. (6) of Ref. 19. Altogether, after having integrated out the fermions, we obtain the grand potential in saddle-point approximation as :

$$\begin{aligned}
 \Omega &= U \sum_i \left( \sum_{\alpha < \alpha'} d_{i,\alpha\alpha'}^2 + 3 \sum_{\alpha < \alpha' < \alpha''} t_{i,\alpha\alpha'\alpha''}^2 + 6q_i^2 \right) \\
 &+ J \sum_i \left( \sum_{\sigma} d_{i,xz\sigma,yz-\sigma}^2 + 3 \sum_{\rho} d_{i,\rho\uparrow,\rho\downarrow}^2 + 4 \sum_{\alpha < \alpha' < \alpha''} t_{i,\alpha\alpha'\alpha''}^2 + 8q_i^2 \right)
 \end{aligned}$$

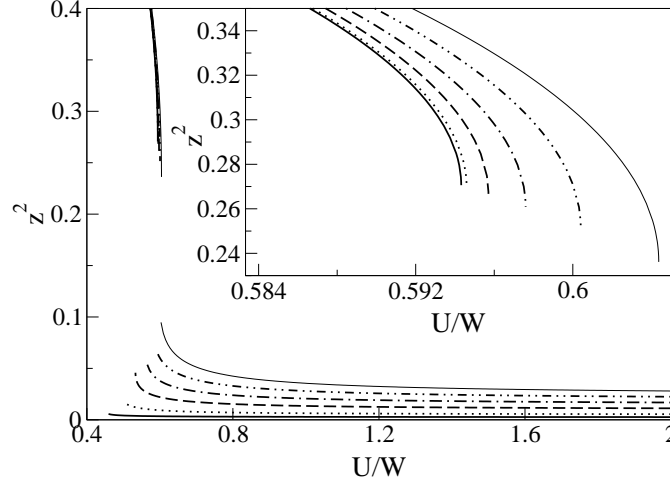


Fig. 2. Effective mass renormalization off half-filling for  $J_H/U = 0.5$  and  $\rho = 2.005$  (full line), 2.01. (dotted line), 2.02 (dashed line), 2.03 (dashed-dotted line), 2.04 (dashed-dotted-dotted line), and 2.05 (thin full line). Inset: Blow up of the “metallic” solutions with the same parameters.

$$\begin{aligned}
 & + \sum_i \lambda_i \left( e_i^2 + \sum_{\alpha} p_{i\alpha}^2 + \sum_{\alpha < \alpha'} d_{i,\alpha\alpha'}^2 + \sum_{\alpha < \alpha' < \alpha''} t_{i,\alpha\alpha'\alpha''}^2 + q_i^2 - 1 \right) \quad (7) \\
 & - \sum_{i,\alpha} \beta_{i,\alpha} \left( p_{i,\alpha}^2 + \sum_{\alpha'} d_{i,\alpha\alpha'}^2 + \sum_{\alpha' \alpha''} t_{i,\alpha\alpha'\alpha''}^2 + q_i^2 \right) \\
 & - \frac{1}{\beta} \sum_{k,\nu,\sigma} \ln \left( 1 + e^{-\beta E_{k,\nu,\sigma}} \right)
 \end{aligned}$$

In a paramagnetic or a ferromagnetic phase, the dispersions are given by :

$$\begin{aligned}
 E_{k,\nu,\sigma} = & \frac{1}{2} \left[ \beta_{xz\sigma} + \beta_{yz\sigma} - 2\mu + \left( z_{xz\sigma}^2 \tilde{e}_k + z_{yz\sigma}^2 \tilde{f}_k \right) + \right. \\
 & \left. + \nu \sqrt{\left( z_{xz\sigma}^2 \tilde{e}_k - z_{yz\sigma}^2 \tilde{f}_k \right)^2 + 4z_{xz\sigma}^2 z_{yz\sigma}^2 \tilde{a}_k^2} \right] \quad (8)
 \end{aligned}$$

where the dependence on  $\sigma$  is only effective in the ferromagnetic phase. Though the resulting mean-field equations only correspond to the saddle-point of an action, the latter gets variationally controlled in the limit of large dimensions<sup>32</sup>. It would be highly desirable to reach the degree of accuracy

### Ferromagnetism in a Realistic Two-Band Model.

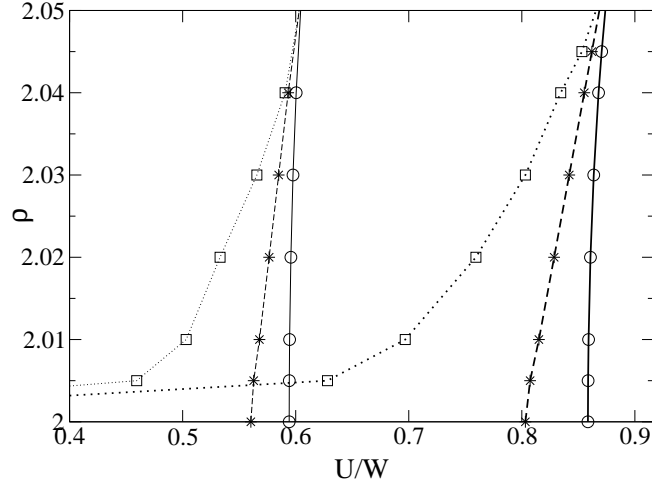


Fig. 3. Coexistence regions of the paramagnetic phases for  $J_H/U = 0.5$  (thin lines) and  $0.3$ , (thick lines). The dashed lines locate the first order transition lines, the dotted lines  $U_{c1}$ , and the full lines  $U_{c2}$ . All lines are guide for the eyes, only.

and reliability of the conserving approximations developed by the Karlsruhe group for impurity models<sup>33,34,35,36</sup>, but to date it appears difficult to extend them to lattice models. Nevertheless mean-field calculations turned out to compare well with numerical simulations<sup>25</sup>, even when calculating the charge structure factor<sup>37</sup>.

### 3. NUMERICAL RESULTS

The saddle-point equations have been solved on a  $800 \times 800$  lattice, at a temperature  $T = t/1000$ . Since the electronic density in the ruthenates under study is  $\rho \sim 2$ , we neglected four-fold occupancies and empty configurations. This approximation is justified in the vicinity of the Mott transition. However it breaks down for densities above three (below one), and for weak coupling, where our results should be taken with care. In particular it results into having a finite effective mass renormalization in the non-interacting limit, which should not be the case. As obtained by Bünemann et al.<sup>38,18</sup>, and Klejnberg and Spalek<sup>39</sup>, the Hund's rule coupling has a strong influence on the Mott transition. While the latter is second order for  $J_H = 0$  and  $\rho = 2$ , or for any  $J_H$  for  $\rho = 1$  or  $3$ , it becomes first order for finite  $J_H$  at half-filling as shown on Fig. 1. The metallic solution

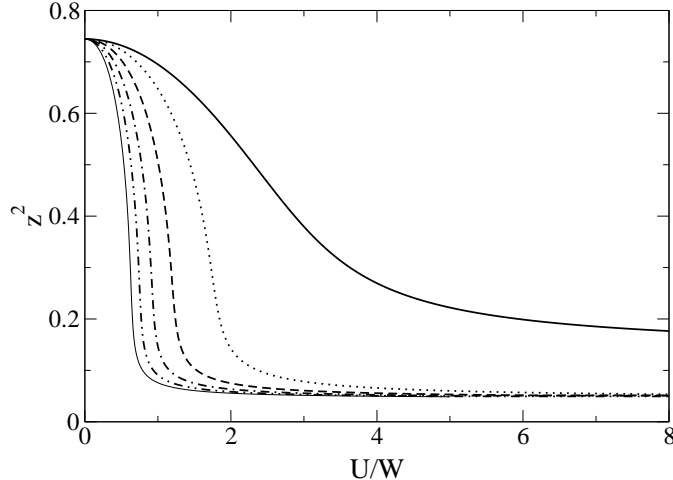


Fig. 4. Effective mass renormalization at  $\rho = 2.1$  for  $J_H/U = 0$  (full line), 0.1 (dotted line), 0.2 (dashed line), 0.3 (dashed-dotted line), 0.4 (dashed-dotted-dotted line), and 0.5 (thin full line).

of the saddle-point equations ceases to exist at a critical value  $U_{c2}$ , without corresponding to a diverging effective mass. Moreover the effective mass is at most renormalized by a factor five for  $J_H/U \geq 0.01$ , in contrast to the one-band case. On top of this metallic solution, there is an insulating paramagnetic solution characterized by a vanishing value of all bosons, but  $d_{xz\uparrow, yz\uparrow}$  and  $d_{xz\downarrow, yz\downarrow}$ , and therefore a diverging effective mass (for finite  $J_H$ ). It extends down to  $U_{c1} = 0$ . We also note that  $U_{c2}$  is slightly larger than  $U_c$ , where the energy of the metallic and insulating solutions coincide. As a result the effective mass renormalization is even more modest in the metallic phase.

Once the system is doped the situation changes little by little. For small electron doping, the first order transition remains but gradually vanishes with increasing electron concentration as shown on Fig. 2. The metallic solution is only modestly affected, except for that it allows for decreasing values of  $z$  in the vicinity of the Mott transition. The insulating solution becomes metallic under electron doping, and the truly insulating state is only found for integer fillings. However the effective mass renormalization remains very large, and accordingly the quasi-particle residue is small. Under these circumstances, the system may well be strongly influenced by other interaction terms, as reviewed by Vollhardt et al.<sup>40</sup>, or disorder effects. This may explain why many transition metal oxides remain insulating even upon



### Ferromagnetism in a Realistic Two-Band Model.

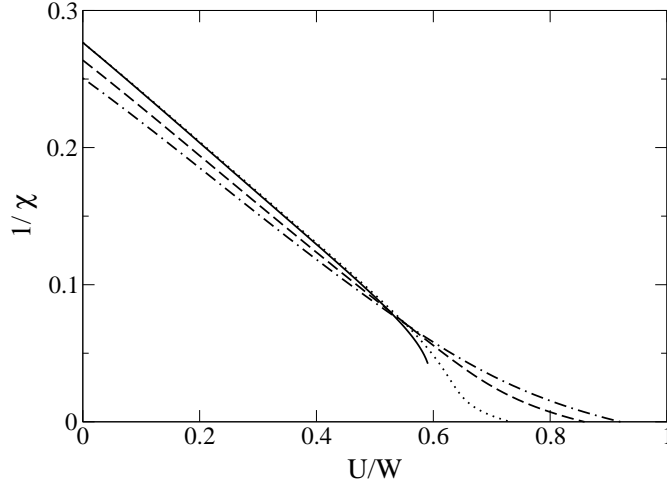


Fig. 5. Inverse magnetic susceptibility for  $J_H/U = 0.5$  and  $\rho = 2$  (full line), 2.1 (dotted line), 2.2 (dashed line), and 2.3 (dashed-dotted line).

substantial doping, such as  $\text{La}_{1-x}\text{Ca}_x\text{VO}_3$ <sup>41</sup>.

When coming from large  $U$ , the "insulating" solution is found to exist down to a critical value  $U_{c1}$ , which is smaller than  $U_{c2}$ . Beside the fact that  $U_{c1} = 0$  at half-filling for any  $J_H$ , it is a complex function of density and  $J_H$  otherwise. It is shown on Fig. 3 for  $J_H/U = 0.3$  and  $0.5$ ; together with  $U_c$  and  $U_{c2}$ . The coexistence region is seen to be largest for  $J_H/U = 0.3$ . It gets somewhat smaller for larger ratio of  $J_H/U$ , but its size drops abruptly for  $J_H/U \rightarrow 0$ . For larger doping the effective mass renormalization is getting a smooth function of  $U$ , as displayed on Fig. 4. Again it strongly depends on  $J_H$ , either in the vicinity of the Mott transition since its location depends on  $J_H$ , or when it is small, even for large  $U$ . Even though the curves are now smooth, one observes that the jumps occurring in the small doping regime are merely replaced by a very sharp drop which is, roughly speaking, separating a good metallic region from a nearly insulating one.

We now switch to the magnetic susceptibility. The latter is obtained by evaluating the Gibbs free energy  $G(m)$  at  $m_1 = 0.1$  and  $m_2 = 0.01$ , and expressing the magnetic susceptibility  $\chi$  as :

$$\chi = \frac{m_1^2 - m_2^2}{2(G(m_1) - G(m_2))} \quad (9)$$

As shown on Fig. 5 for  $J_H/U = 0.5$  the spin susceptibility does not diverge at half-filling, regardless of the value of  $J_H$ , though it is strongly renormalized at the Mott transition, where the curve stops. In the "metallic"

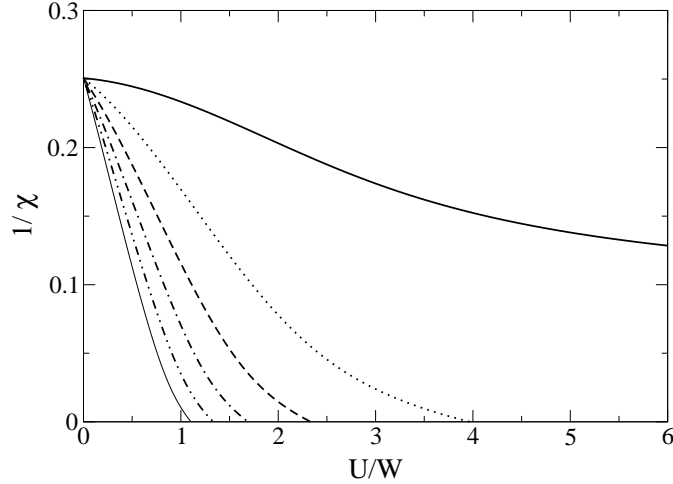


Fig. 6. Inverse magnetic susceptibility for  $\rho = 2.3$  and  $J_H/U = 0$  (full line), 0.1 (dotted line), 0.2 (dashed line), 0.3 (dashed-dotted line), 0.4 (dashed-dotted-dotted line), and 0.5 (thin full line).

regime, as defined above, the renormalization is slightly but increasingly suppressed with increasing electron doping. Nevertheless, in this metallic regime, there is no divergence of  $\chi$ , but merely a renormalization of it by at most a factor five. This renormalization is comparable to the one of the effective mass, though somewhat larger.

As one might anticipate, the Hund's rule coupling has a strong influence on the magnetic susceptibility, as shown on Fig. 6, where we display the inverse magnetic susceptibility as a function of the interaction strength for several values of  $J_H/U$ , at fixed density  $\rho = 2.3$ . For  $J_H = 0$ ,  $\chi$  is barely affected by the interaction, and is not found to diverge for  $U$  up to  $10W$ . Diverging susceptibilities start to appear once the Hund's rule coupling is finite. The critical value of  $U$  decreases with increasing ratio  $J_H/U$ , but always stays above  $U_c$ . We therefore have no evidence for a weakly renormalized ferromagnetic system. This is in agreement with the one-band Hubbard model, where a ferromagnetic ground state only takes place for very large interaction strengths and moderate hole doping<sup>42</sup>.

The instabilities of the paramagnetic phases are collected on Fig. 7, for several values of  $J_H/U$ . The range of stability of the paramagnetic phase is seen to depend weakly on density for large ratio of  $J_H/U$ . In contrast, it may extend to large interaction strengths for  $J_H/U = 0.1$ . On top there is a strong asymmetry around  $\rho = 2.5$ , which is more a consequence of the

### Ferromagnetism in a Realistic Two-Band Model.

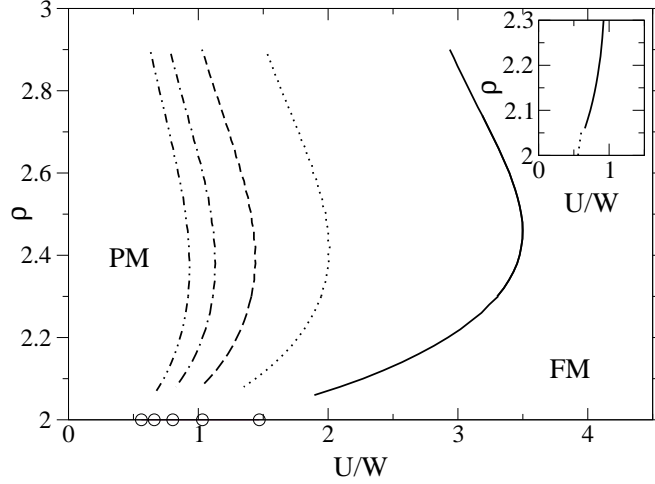


Fig. 7. Instability line towards ferromagnetism in the density- $U$  plane for  $J_H/U = 0.1$  (full line),  $0.2$  (dotted line),  $0.3$  (dashed line),  $0.4$  (dashed-dotted line), and  $0.5$  (dashed-dotted-dotted line). The circles are indicating the corresponding  $U_c$ 's at half-filling. Inset: Instability line (full line), and first order transition line (dotted line), for  $J_H/U = 0.5$ .

difference between  $U_c$  for  $\rho = 2$  and  $\rho = 3$  (see Ref. 43), than a consequence of neglecting four-fold occupancy. The choice  $m_1 = 0.1$  in Eq. (9) results into a somewhat overestimated stability range for the paramagnetic phase, but numerical instabilities appear when working with smaller values for  $m_1$ . As displayed in the inset of Fig. 7, the instability lines connect to the first order transition line separating two paramagnetic solutions, where the latter ends, within numerical accuracy. No ferromagnetic solution with magnetization  $m_1$  has been found for very small doping and  $U > U_c$ .

When comparing this phase diagram to La-doped  $\text{Ca}_2\text{RuO}_4$ , we see that a small amount of electron doping turns a Mott insulator into a ferromagnet, in agreement with experiment<sup>4</sup>. However the shape of the instability lines does not appear to be compatible with the experimental situation met in La-doped  $\text{Sr}_2\text{RuO}_4$ . Indeed no instability line extends to the very vicinity of half-filling in the metallic regime. This point may be easily overcome by noticing that the band involving the  $d_{xy}$  orbital is not completely filled<sup>16,12</sup>, but only carries about 1.8 electrons per Ru atom. One should therefore concentrate on the vicinity of  $\rho = 2.2$ . But then, increasing the electron density from  $\rho = 2.2$  at fixed ratio  $U/W$  does not allow for going from a paramagnetic state to a ferromagnetic one.

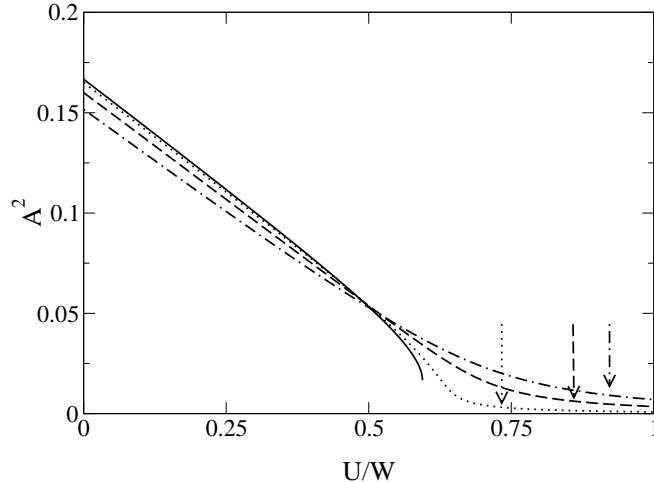


Fig. 8. Double occupancy in the same orbital for  $J_H/U = 0.5$  and  $\rho = 2$  (full line), 2.1 (dotted line), 2.2 (dashed line), and 2.3. The arrows indicate the location of the corresponding ferromagnetic instabilities.

In order to reconcile the theoretical and experimental data, one would therefore need to assume that La doping not only changes the electronic density, but also strongly influences (reduces) the band width. An argument pointing towards this direction is provided by a recent structural study by Friedt *et al.*<sup>44</sup>, which clearly points out that the structural parameters of the ruthenates may easily vary to a large extent, even under a temperature change. There is little doubt that this holds for the energy levels  $\epsilon_d$  and  $\epsilon_p$  and the overlap integrals, and therefore for the band width. Recalling that the ionic radius of  $\text{La}^{3+}$  and  $\text{Ca}^{2+}$  are very similar, one may expect that La doping indeed induces a reduction of the band width, since Ca substitution does it, leading to a ferromagnetic instability. Another reason for the discrepancy may follow from considering the  $d_{xy}$  band for self-doping only, instead of including it in its own right into the calculation from the outset. According to a recent work by Anisimov *et al.*<sup>45</sup>, it indeed seems to play an important role.

Since the four-fold occupancy turned out to be negligible, one may wonder whether further simplifications could be introduced without qualitatively altering the results. Indeed the determination of the saddle-point, even in the simplest paramagnetic approximation is not an easy task, and, except for the non-interacting and  $J_H = 0$  limits, quite careful numerical work is required. To address this question, we are displaying the less probable dou-

### Ferromagnetism in a Realistic Two-Band Model.

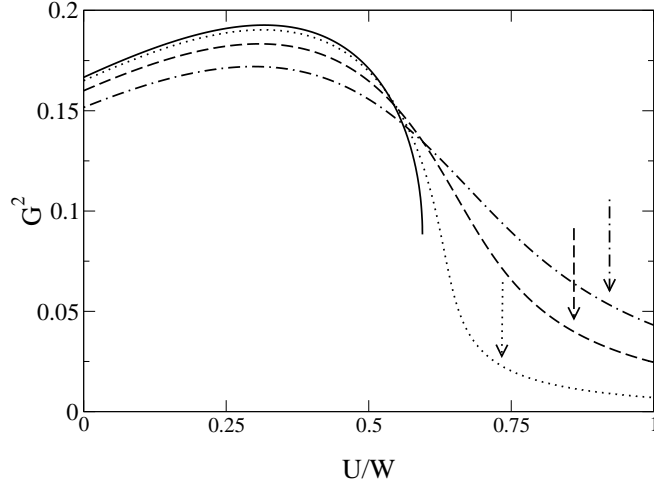


Fig. 9. Double occupancy in different orbitals with opposite spin projections for  $J_H/U = 0.5$  and  $\rho = 2$  (full line), 2.1 (dotted line), 2.2 (dashed line), and 2.3. The arrows indicate the location of the ferromagnetic instabilities.

ble occupancies on Fig. 8 and 9. After introducing :  $A^2 \equiv d_{xz\uparrow,xz\downarrow}^2 + d_{yz\uparrow,yz\downarrow}^2$  and  $G^2 \equiv d_{xz\uparrow,yz\downarrow}^2 + d_{xz\downarrow,yz\uparrow}^2$ , we see that they behave quite differently as a function of  $U$  and  $J_H$ . Indeed the double occupancy in the same orbital ( $A^2$ ), which is corresponding to the largest local interaction is suppressed monotonically under an increase of  $U$ . It nevertheless keeps a substantial value in the metallic regime, where it may therefore not be neglected. In contrast it becomes very small in the vicinity of the ferromagnetic instability, and presumably neglecting  $A$  is not going to have a strong influence on the determination of the instability line, especially in the large  $J_H$  regime.

The double occupancy in different orbitals with  $S_z = 0$  ( $G^2$ ) behaves quite differently as shown on Fig. 9. An increase of  $U$  enhances it in about the entire metallic region. It then sharply drops in the vicinity of the Mott transition, but (except for the very vicinity of the Mott insulating state) its value remains quite sizeable, even for strong Hund's rule interaction and large  $U$ . We therefore conclude that even the instability line cannot be accurately obtained by setting  $G = 0$ , in contrast to  $A$ . That such an approximation, (which is corresponding to the limit  $J_H \rightarrow \infty$ ) will strongly influence the instability line is not particularly amazing, since the latter does depend on  $J_H$ . But this study shows that the dependence mostly arises through  $G$ , while the impact of  $A$  is far smaller. Therefore the precise value of the parameter  $U_3$  in Eq. (4) is only marginally relevant.

#### 4. CONCLUSION

In summary we have investigated a two-band Hubbard model with a realistic band structure, where no van Hove singularity appear at, or in the vicinity of, half band filling. We have shown that the first order metal to insulator transition that occurs at half-filling first extends to small but finite doping in a strict sense, and second only weakly smears out for larger doping. This divides the phase diagram into a “metallic” region, where the effective mass is only weakly renormalized and no ferromagnetic instability is found, and an “insulating” region, where the effective mass is strongly renormalized, and ferromagnetism is found. On top, there is a surprisingly small region in-between, which is interpolating between these two behaviors.

#### ACKNOWLEDGMENTS

It is our great pleasure to dedicate the present paper to Prof. Peter Wölfle on the occasion of his 60th birthday, especially one of us (RF) is warmly thanking him for having been introduced to the field of slave boson theories. We are very grateful to V. Dobrosavljevic for having suggested this work, and for numerous discussions, and to H. Beck for interesting discussions. We acknowledge the financial support by the fonds national suisse de la recherche scientifique.

#### REFERENCES

1. Y. Maeno, H. Hashimoto, K. Yoshida, S. Nishizaki, T. Fujita, J. G. Bednorz, and F. Lichtenberg, *Nature (London)* **372**, 532 (1994).
2. G. Cao, S. McCall, M. Shepard, J. E. Crow, and R. P. Guertin, *Phys. Rev. B* **56**, R2916 (1997).
3. A. V. Puchkov, M. C. Schabel, D. N. Basov, T. Startseva, G. Cao, T. Timusk, and Z. X. Shen, *Phys. Rev. Lett.* **81**, 2747 (1998).
4. G. Cao, S. McCall, V. Dobrosavljevic, C. S. Alexander, J. E. Crow, and R. P. Guertin, *Phys. Rev. B* **61**, R5053 (2000).
5. G. Cao and V. Dobrosavljevic, Private communication.
6. G. Cao *et al.*, unpublished.
7. M. Eschrig, J. Ferrer, and M. Fogelström, *Phys. Rev. B* **63**, 220509(R) (2001).
8. *Proc. of the Yamada Conference LI, "The International Conference on Strongly Correlated Electron Systems"*, edited by K. Miyake, H. Harima, H. Kohno, T. Saso, H. Sato, R. Settai, and Y. Onuki, Nagano, Japan (1999), Y. Maeno, *Physica B* **281&282**, 865 (2000).
9. M. Sigrist, D. Agterberg, A. Furusaki, C. Honerkamp, K. K. Ng, T. M. Rice, and M. E. Zhitomirsky, *Physica C* **317-318**, 134 (1999).

## Ferromagnetism in a Realistic Two-Band Model.

10. G. Baskaran, *Physica B* **222&223**, 490 (1996).
11. T. M. Rice and M. Sigrist, *J. Phys.: Condens. Matt.* **7**, L643 (1995).
12. C. Noce and M. Cuoco, *Phys. Rev. B* **59**, 2659 (1999).
13. A. P. Mackenzie, S. R. Julian, A. J. Diver, G. G. Lonzarich, Y. Maeno, S. Nishigaki, and T. Fujita, *Phys. Rev. Lett.* **76**, 3786 (1996).
14. M. Schmidt, T. R. Cummins, M. Bürk, D. H. Lu, N. Nücker, S. Schuppler, and F. Lichtenberg, *Phys. Rev. B* **53**, R14 761 (1996).
15. T. Oguchi, *Phys. Rev. B* **51**, 1385 (1995).
16. D. J. Singh, *Phys. Rev. B* **52**, 1358 (1995).
17. S. Sugano, Y. Tanabe, and H. Kamimura, *Multiplets of Transition-Metal Ions in Crystals*. Pure and Applied Physics **33**, Academic Press, New York, 1970.
18. J. Bünnemann, W. Weber, and F. Gebhard, *Phys. Rev. B* **57**, 6896 (1998).
19. R. Frésard and G. Kotliar, *Phys. Rev. B* **56**, 12909 (1997).
20. V. Dorin and P. Schlottmann, *Phys. Rev. B* **47**, 5095 (1993).
21. H. Hasegawa, *J. Phys. Soc. Jpn.* **66**, 1391 (1997).
22. G. Kotliar and A. E. Ruckenstein, *Phys. Rev. Lett.* **57**, 1362 (1986).
23. T. C. Li, P. Wölfle, and P. J. Hirschfeld, *Phys. Rev. B* **40**, 6817 (1989).
24. R. Frésard and P. Wölfle, *Int. J. Mod. Phys. B* **6**, 685 (1992).
25. R. Frésard, M. Dzierzawa, and P. Wölfle, *Europhys. Lett.* **15**, 325 (1991).
26. R. Frésard and P. Wölfle, *J. Phys.: Condens. Matt.* **4**, 3625 (1991).
27. E. Arrigoni and G. C. Strinati, *Phys. Rev. B* **44**, 7455 (1991).
28. H. Hasegawa, *Phys. Rev. B* **56**, 1196 (1997).
29. I. Yang, E. Lange, and G. Kotliar, *Phys. Rev. B* **61**, 2521 (2000).
30. Proceedings of the NATO ARW “The Hubbard Model: Its Physics and Mathematical Physics”, edited by D. Baeriswil, D. K. Campbell, J. M. P. Carmelo, F. Guinea, and E. Louis, San Sebastian (1993), R. Frésard and K. Doll, *Plenum*, 385 (1995).
31. H. Hasegawa, condmat/0005271.
32. J. Bünnemann, F. Gebhard, and W. Weber, *J. Phys.: Condens. Matt.* **9**, 7343 (1997).
33. J. Kroha and P. Wölfle, condmat/0105491.
34. J. Kroha, P. J. Hirschfeld, K. A. Muttalib, and P. Wölfle, *Solid State Commun.* **83**, 1003, (1992).
35. J. Kroha, P. Wölfle, and T. A. Costi, *Phys. Rev. Lett.* **79**, 261 (1997).
36. J. Kroha and P. Wölfle, *Acta Phys. Pol. B* **29**, 3781 (1998).
37. W. Zimmermann, R. Frésard, and P. Wölfle, *Phys. Rev. B* **56**, 10 097 (1997).
38. J. Bünnemann and W. Weber, *Phys. Rev. B* **55**, 4011 (1997).
39. A. Klejnberg and J. Spalek, *Phys. Rev. B* **57**, 12 041 (1998).
40. D. Vollhardt, N. Blümer, K. Held, M. Kollar, J. Schlipf, and M. Ulmke, *Z. Phys. B* **103**, 283 (1997).
41. H. C. Nguyen and J. B. Goodenough, *Phys. Rev. B* **52**, 8776 (1995).
42. B. Möller, K. Doll, and R. Frésard, *J. Phys.: Condens. Matt.* **5**, 4847 (1993).
43. J. P. Lu, *Phys. Rev. B* **49**, 5687 (1994).
44. O. Friedt, M. Braden, G. André, P. Adelman, S. Nakatsuji, and Y. Maeno, *Phys. Rev. B* **63**, 174432 (2001).
45. V. I. Anisimov, I. A. Nekrasov, D. E. Kondakov, T. M. Rice, and M. Sigrist, condmat/0107095.